

ESTIMATION OF DAILY ENERGY GAIN OF SOLAR TRACKING SURFACES BASED ON GEOGRAPHIC POSITION

¹Higor Miguel

²Leticia Colombi Gomes

³Cesar Turczyn Campos

^{4*}Pablo Rodrigues Muniz

¹Federal Institute of Espírito Santo – *Campus* Vitória. E-mail: higor.mig@gmail.com

²Federal Institute of Espírito Santo – *Campus* Vitória. E-mail: leticiacolombi@outlook.com

³Federal Institute of Espírito Santo – *Campus* Vitória. E-mail: cesar.turczyn@ifes.edu.br

⁴Federal Institute of Espírito Santo – *Campus* Vitória. E-mail: pablrom@ifes.edu.br

*Corresponding author

Manuscript submitted on 11/10/2020, accepted on 03/10/2021 and published on 04/15/2021.

Abstract: The performance of solar systems depends on the effective incident solar energy on the capture surface. This factor is dependent on the geographic position, the orientation of the surface, atmospheric conditions, and other geo-climatic factors. Solar trackers, typically uni- and biaxial, are used to optimize the capture of solar radiation via movement of the plane of incidence of these devices. A reliable estimation of the energy gain of these trackers with respect to a fixed surface facilitates more accurate analyses of the feasibility, operation, and maintenance of solar ventures. In this work, a method for estimating the relative energy gain of uni- and biaxial solar trackers is developed. This approach applies to locations between the Arctic Circle and the Antarctic Circle, using geographic coordinates and the altitude of the location of interest, providing daily results throughout the year. Unlike empirical results or case studies, the proposed method applies to any location and has a low error. It can be implemented using iterative algorithms with a low computational cost and can be easily utilized by researchers and technicians in the field.

Keywords: solar energy; solar trackers; energy capture.

1 INTRODUCTION

With population growth and the expansion of industries and businesses, it is necessary to invest in research and development in the clean and renewable energy sector, with the main objective of facilitating sustainable socio-economic development. In this respect, solar energy systems have attracted increasing attention because the generated energy is essentially unlimited in addition to being free from pollution and noise (BAGGIO, 2016).

To maximize the effective intensity of the solar radiation that is incident on the plane wherein solar energy is converted into electrical or thermal energy, several mechanisms are utilized. Some researchers have studied interventions on external elements of solar energy systems, in order to increase their efficiency. (XU et al., 2018) added external lenses to photovoltaic thermal (PV/T) systems, increasing the output power by 29%. Other researchers have evaluated the issue of the orientation

of the energy collecting surfaces. (UNGURESAN et al., 2017) studied the orientation of building facades in order to capture solar energy and convert it to another form of energy. They found that depending on the location and the type of final energy (heat, cold or electrical), a specific facade can produce since almost zero to something close to 70% of the capacity of the four facades together.

Maximizing the effective intensity of solar energy on the surface includes the movement of the plane of incidence, and the optimization of the capture of solar energy by continuously positioning the surface towards the Sun. In these mechanisms, tracking surfaces follow the path of the sun to minimise the angle of incidence. They are classified according to the degrees of freedom of rotation that is allowed, and can be one axis (uniaxial), or two axes (biaxial) (HAFEZ; YOUSEF; HARAG, 2018; RECA-CARDEÑA; LÓPEZ-LUQUE, 2018), with continuous or daily adjustment (BROWNSON, 2014; DUFFIE; BECKMAN, 1985).

These tracker surfaces are further sub-classified according to the type of adjustment that is used into continuous or daily. Tracking surfaces with continuous adjustment vary their angle of incidence throughout the day. Those with daily adjustment are set at a maximum incidence angle during solar noon (BROWNSON, 2014; DUFFIE; BECKMAN, 1985). In order to analyse the maximum radiation uptake in relation to the number of axes of rotation, only the first type of tracking will be considered.

Solar energy capture gain from using solar trackers has already been investigated in several studies. Bahrami et al. (2016) utilized six types of solar trackers in cities with different. The authors used mathematical models to estimate the intensity of solar energy available on a perfect surface that is continuously directed towards the incident solar radiation, and performed experiments to record and analyse the available solar

energy on surfaces controlled by solar trackers (BAHRAMI; OKOYE; ATIKOL, 2016). Nonetheless, mathematical models have not been developed to estimate the available solar energy of receiving surfaces and solar trackers.

Other authors have used experimental approaches to compare the energy captured by fixed surfaces to the energy captured by surfaces mounted on solar trackers (ABDELGHANI-IDRISSI et al., 2018; AL-RAWAHI; AL-AZRI, 2019; AWASTHI et al., 2020; BATAYNEH et al., 2019; CLIFFORD; EASTWOOD, 2004; FATHABADI, 2016; KASBURG; FRIZZO STEFENON, 2019; SIDEK et al., 2017; ZHU; LIU; YANG, 2020). The results were specific to the location and study conditions in general, and indicate that the annualised gain for the capture of solar energy is approximately 13% to 40% for uniaxial solar trackers and up to 60% for biaxial trackers, compared to a fixed surface. This problem was investigated using a simpler approach in several studies, in which typical values and the curves of the energy capture gain were utilized (DE MACEDO; SALDIAS; ANDO JUNIOR, 2016).

It should be noted that these published studies did not include models for the estimation of the gain associated with solar energy capture using solar trackers based on variables of interest such as local latitude and day of the year. Moreover, these investigations were predominantly experimental studies performed in specific locations, and typically cannot be used for performance estimation in other locations.

Software are available for estimating the capture of solar energy by plans, similarly to the purpose of this article. (ALLAM, 2017) analysed some of them and wrote a white paper summarizing their features. HOMER PRO, developed by NREL (National Renewable Energy Laboratory), yields not so comprehensive and detailed PV electricity generation report due to limited information on

weather data, as well as it does not add may loss factors during PV power generation. PV F-CHART, developed in University of Wisconsin, makes difficult to quickly compare generation data by switching location. It seems to be not suitable for calculation of PV power in actual conditions. There is no option to import weather data from common sources. On the other hand, PVPLANNER, provided by SolarGis, claims their data is highly accurate and offers a rigorous systematic validation approach. However, there is no option of importing weather data from other sources. PVSYST, developed by physicist Andre Mermoud and electrical engineer Michel Villoz claims to be used by architects, engineers, researchers, and students. It estimates energy production in a detailed way, with hourly estimations. RETSCREEN, developed by National Resources Canada, uses weather data from NASA database but does not allow adding other data sources or custom data. SAM (System Advisor Model), developed by the U.S. Department of Energy (DoE) and the National Renewable Energy Laboratory (NREL), can be worked upon several weather database. However, it is based on US data and energy policies, so it may not be suitable worldwide. SOLAR PRO may be the only software that offers a minute-by-minute calculation. Besides being user-friendly, it is not possible to add weather database. In short, these software are not open-source code and use specific databases, hindering its use throughout the world.

To address these limitations, this study aims to mathematically model the solar energy that is incident on fixed flat surfaces, uniaxial solar trackers, and biaxial solar trackers, for typical situations involving solar energy capture systems, according to the local latitude, date, and time. This model, subject to changes and improvements, allows the use of any database of solar radiation desired by the user, and it will facilitate a comparison of

the energy gain obtained among the different types of planes, depending on the location of interest and time of the year. In addition to scientific knowledge, the model will allow for a more accurate economic assessment of solar energy projects, as well as better operation management and maintenance intervention, given that the installed system may exhibit an expected performance chart in terms of energy gain for the entire year.

This paper consists of five sections. The introductory section describes the research problem that is subsequently addressed. In section 2 (Methods), the mathematical tools for estimating the solar energy that is incident on a flat surface according to its location, date and time are presented. Section 3 (Calculation) is a description of the model based on a computational approach in addition to the results for the performed tests. Section 4 (Results) is a summary of the results and energy analysis for flat surfaces, in addition to uni- and biaxial solar trackers for locations at different latitudes. Finally, the conclusions section highlights the advances and potential of the proposed method.

2 METHODS

2.1 SOLAR ENERGY TRAJECTORY

Solar Constant (SC) is the intensity of solar energy across the electromagnetic spectrum that crosses an unit area perpendicular to the direction of the solar beam outside the Earth's atmosphere, per unit time (PAP, 1986). It is referred to as the total solar irradiance (TSI) due to the fluctuation of this value so that SC is currently defined as the long-term average value of the TSI (FRÖHLICH; LEAN, 2004; GUEYMARD, 2018; KUHN; ARMSTRONG, 2004; USOSKIN, 2017). Nowadays, the value of SC is estimated to be $1,361.1 \pm 5 \text{ W/m}^2$ (GUEYMARD, 2018).

2.2 ASTRONOMIC MOVEMENTS AND THEIR INFLUENCES ON EXTRATERRESTRIAL SOLAR ENERGY

The Earth revolves around the Sun in an elliptical orbit with the Sun at one of the focal points, which despite its small eccentricity, influences the solar energy that reaches Earth's surface (BROWNSON, 2014). In order to obtain an accurate Earth-Sun distance, (IQBAL, 1983) highlighted Spencer's work (BRAUN; MITCHELL, 1983), in which an equation was derived to correct for the eccentricity with a maximum error of 0.0001 rad (Eq. 1).

$$E_0 = 1.000110 + 0.034221 \cos(\Gamma) + 0.001280 \sin(\Gamma) + 0.000719 \cos(2\Gamma) + 0.000077 \sin(2\Gamma) \text{ [rad]} \quad 1$$

In Eq. 1, Γ represents the day angle that is calculated using Eq. 2 (SPENCER, 1971).

$$\Gamma = 2\pi \left(\frac{d_n - 1}{365} \right) \text{ [rad]} \quad 2$$

Multiplying E_0 by the Solar Constant, the irradiance that reaches the top of the Earth's atmosphere is obtained for day d_n .

Another factor that influences the solar energy incident on the Earth is the declination of its axis. From an astronomical perspective, there are two relevant planes associate with the Earth's trajectory around the Sun; the orbit plane called the Ecliptic plane and the plane that cuts across the equator of the Earth, i.e. the plane of the Celestial Equator (SPROUL, 2007).

Perpendicular to the Celestial Equator is the Earth's axis of rotation, known as the polar axis. With respect to the Ecliptic plane, the Polar Axis has a small inclination of approximately 23.45° (IQBAL, 1983; PINHO; GALDINO, 2014). Although it does not change during the year, the angle between the Ecliptic and Equatorial planes changes. This angle is called the Solar Declination (δ) (IQBAL,

1983), that can be calculated through Eq. 3 (SPENCER, 1971).

$$\delta = 0.006918 - 0.399912 \cos(\Gamma) + 0.070257 \sin(\Gamma) - 0.006758 \cos(2\Gamma) + 0.000907 \sin(2\Gamma) - 0.002697 \cos(3\Gamma) + 0.001480 \sin(3\Gamma) \text{ [rad]} \quad 3$$

For developing this work, as well as other studies based on the variation of solar energy over a given period of time, the use of Solar Time (ST) is necessary. This time is measured with respect to the Sun crossing and the reference meridian of the observer located between the meridians that define the time zone for a region. It is computed from Eq. 4 (IQBAL, 1983).

$$ST - Local Time = 4(L_{ref} - L_{local}) + 229.18 E_t \quad 4$$

[min]

Where E_t is a correction due to fluctuation of the duration of a day calculate from Eq. 5 (SPENCER, 1971), L_{ref} is the reference longitude, and L_{local} is the local longitude.

$$E_t = 0.0000075 + 0.001868 \cos(\Gamma) - 0.032077 \sin(\Gamma) - 0.014615 \cos(2\Gamma) - 0.040849 \sin(2\Gamma) \text{ [rad]} \quad 5$$

2.3 SOLAR GEOMETRY AND THE ESTABLISHMENT OF EXTRATERRESTRIAL IRRADIANCE

The key angles of the solar incidence geometry are the zenith (θ_z), solar altitude (α_s), time (ω), solar azimuth (γ_s), azimuth (γ), surface slope (β), and the incidence (θ) (BROWNSON, 2014; DUFFIE; BECKMAN, 1985; IQBAL, 1983).

The angles that are independent of the type of surface on which the radiation is incident are those that depend only on the geographic and spatial position of the observer. As such, they are based only on the latitude, longitude, and declination of the terrestrial axis. These are the zenith, solar altitude, time, and solar azimuth angles (BROWNSON, 2014).

After converting local time to Solar Time (ST), a conversion from time in

hours to angle in radians is performed according to Eq. 6 (IQBAL, 1983).

$$\omega = (ST - 12) \frac{\pi}{12} [\text{rad}] \quad 6$$

Given that the solar altitude is a complementary angle relative to the zenith, for a given geographic position, using the relationship between the centre of the solar disk and the horizontal surface where the observer is located, it is possible to describe both the zenith angle and the angle of solar altitude. The relationship is represented by Eq. 7 (BRAUN; MITCHELL, 1983).

$$\cos(\theta_z) = \sin(\varphi) \sin(\delta) + \cos(\varphi) \cos(\delta) \cos(\omega) = \sin(\alpha_s) \quad 7$$

In spite of the assumption that a value is within the tropics, there is a relationship between the solar azimuth angle and the hour angle. Both yield negative angular values prior to solar noon and positive values thereafter. To correct the errors related to latitude and solar declination, the sign of the solar azimuth angle should follow the sign of the hour angle (Eq. 8) (DUFFIE; BECKMAN, 1985).

$$\gamma_s = \text{sign}(\omega) \left| \cos^{-1} \left(\frac{\cos(\theta_z) \sin(\varphi) - \sin(\delta)}{\sin(\theta_z) \cos(\varphi)} \right) \right| \quad 8$$

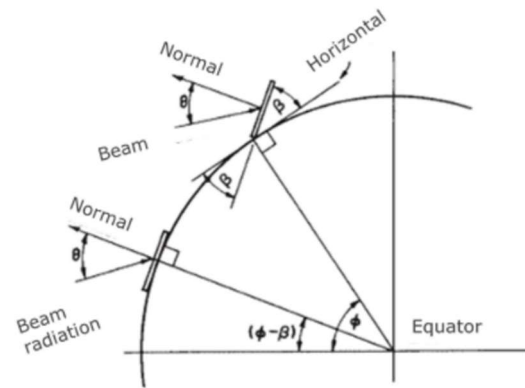
On fixed surfaces, the azimuth angle, the slope of the surface, and the angle of incidence represent the three angles that vary according to the type of inclined flat surface. The surface slope is generally a known variable for fixed installations, in contrast to the azimuth and incidence angles, which are calculated quantities.

Given that the Earth is relatively symmetrical with regard to the equator, it is noted that the angle of incidence is the same for both situations, which implies that the inclination of the plane of incidence compensates for the inclination of the local latitude. In addition, the latitude-slope set is defined as $\varphi - \beta$ in the

Northern Hemisphere and $\varphi + \beta$ in the Southern Hemisphere. Considering that a southern latitude is conventionally defined as negative, the angle of incidence can be given by Eq. 9 (DUFFIE; BECKMAN, 1985). Figure 1 shows these angles for planes at the Equator.

$$\cos(\theta) = \frac{\sin(\delta) \sin(\varphi - \beta) + \cos(\delta) \cos(\varphi - \beta) \cos(\omega)}{\cos(\omega)} \quad 9$$

Figure 1: Normal incidence for planes pointed at the Equator



(DUFFIE; BECKMAN, 1985).

The most common continuous uniaxial tracking method of the Sun is one in which the rotation angle is taken from the north-south axis. The plane has an optimised inclination according to the installation location (close to the latitude, generally), and tracking is realised from east to west. This approach aims to minimise the angle of incidence for the case of $\cos(\theta) \approx \cos(\delta)$. In this case, the absolute inclination and the azimuth angle of the plane of incidence vary continuously and can be determined using Eq. 10 and 11 (DUFFIE; BECKMAN, 1985).

$$\gamma = \tan^{-1} \left(\frac{\sin(\theta_z) \sin(\gamma_s)}{\cos(\theta') \sin(\varphi)} \right) + \pi C_1 C_2 [\text{rad}] \quad 10$$

such that we have:

$$\cos(\theta') = \cos(\theta_z) \cos(\varphi) + \sin(\theta_z) \sin(\varphi) \cos(\gamma_s)$$

$$\begin{cases} C_1 = 0, & \text{if } \gamma = \tan^{-1} \left(\frac{\sin(\theta_z) \sin(\gamma_s)}{\cos(\theta') \sin(\varphi)} \right) \gamma_s \geq 0 \\ C_1 = 1, & \text{if } \gamma = \tan^{-1} \left(\frac{\sin(\theta_z) \sin(\gamma_s)}{\cos(\theta') \sin(\varphi)} \right) \gamma_s < 0 \end{cases}$$

$$\begin{cases} C_2 = 1, & \text{if } \gamma_s \geq 0 \\ C_2 = -1, & \text{if } \gamma_s < 0 \end{cases}$$

$$\tan(\beta) = \frac{\tan(\varphi)}{\cos(\gamma)} \quad 11$$

For two-axis tracking surfaces, continuous adjustment ensures that regardless of the time of day and day of the year, the incidence angle is always normal to the surface i.e., the angle of incidence is 0 (zero). For this purpose, $\gamma = \gamma_s$ and $\beta = \theta_z$ are applied in Eq. 9 (BRAUN; MITCHELL, 1983). Thus, it is simplified as follows:

$$\begin{aligned} \cos(\theta) &= \cos(\theta_z) \cos(\theta_z) + \sin(\theta_z) \sin(\theta_z) \\ \cos(\theta) &= \cos^2(\theta_z) + \sin^2(\theta_z) = 1 \end{aligned}$$

2.3.1 Establishment of extra-terrestrial solar irradiance

Considering a surface with a slope β and an incident solar radiation of I_{cs} , the line that represents the direction and orientation of the incidence of solar radiation and the normal line to the plane I_{inst} form the angle of incidence θ (IQBAL, 1983).

The irradiance at the top of the Earth's atmosphere for one hour can be calculated by multiplying the solar constant by a correction factor to account for the eccentricity of the Earth's orbit and the angle of incidence in the plane at the moment of interest, as observed in Eq. 12 (DUFFIE; BECKMAN, 1985).

$$I = I_{cs} E_0 \cos \theta \text{ [Wh/m}^2\text{]} \quad 12$$

2.4 ATMOSPHERIC ATTENUATIONS OF SOLAR RADIATION

The radiation that reaches the Earth's surface depends directly on the concentration of ozone, water vapour, aerosols, and clouds that form the atmosphere. The concentration of these elements in the short term varies randomly, causing considerable changes in the structure of the atmosphere (IQBAL, 1983).

2.4.1 Air mass

The term air mass (AM) describes the effective share of the atmosphere that solar radiation must traverse to reach a certain point on the ground. The greater the stretch of the atmosphere covered by the sun's rays, the greater the dispersion and absorption (DUFFIE; BECKMAN, 1985).

The AM value can be approximated using the model proposed by Kasten and Young (1989) which is represented by Eq. 13 (RIGOLLIER; BAUER; WALD, 2000).

$$\begin{aligned} AM(\theta_z) &= \frac{e^{-\frac{h}{AR}}}{\cos(\theta_z) + 0,50572 (6,07995 + 90 - \theta_z)^{-1,6364}} \quad 13 \end{aligned}$$

2.4.2 Atmospheric attenuation - Clear sky models

The attenuation due to the atmosphere varies not only with the angle of penetration i.e., according to the variations of the air mass, but also occurs with changes of the atmospheric conditions such as changes in water vapour concentrations, ozone, and dust. Therefore, it is important to define a pattern in which solar radiation reaches the Earth's surface under "normal conditions" in that period (DUFFIE; BECKMAN, 1985).

In this case, Clear-Sky models are used, which involves the estimation of the solar irradiance on Earth during the crossing a "clear sky," with the objective of simplifying the equations of atmospheric attenuation using relatively simple parameterizations (ANTONANZAS-TORRES et al., 2019).

One of the simplest Clear-Sky models was developed by Meinel (1977), which is based only on the solar geometry. Although a high precision was not obtained in Behar's research (BEHAR et al., 2019), the simplicity of the method (depends only on the value of the air mass) is quite appealing. Eq. 14 represents this model mathematically.

$$B = I \times 0,7^{AM^{0,678}} \text{ [Wh/m}^2\text{]} \quad 14$$

Given that the relative gain for the capture of solar energy by a solar tracking surface with respect to a fixed surface is practically constant for the variation of the sky clearance factor (AL-RAWAHI; AL-AZRI, 2019), and given that this work aims to develop a model that facilitates a comparison of different types of solar energy capture surfaces when subjected to the same conditions, the Meinel Model will be adopted to estimate atmospheric attenuation.

Due to the role of direct radiation (COFFARI, 1977), given the type of atmospheric modelling chosen (clear-sky) and the comparative nature of this work, only the direct part of the radiation will be addressed.

3 CALCULATION

3.1 SCOPE AND CONSTRAINTS

All the equations introduced in this investigation are directly or indirectly based on trigonometric functions. When working with these types of functions, the data modelling automatically incurs mathematical uncertainties, for instance, in the case of latitudes of poles (90°). As such, there was an attempt to address these uncertainties. Nevertheless, the uncertainty could not be eliminated, such as the uncertainty that occurs for latitudes greater than 66.5° (in magnitude). This occurs because sunrise and sunset determinations. Without this equation, it is not possible to define the beginning and end of the day and, consequently, the irradiance.

This indeterminacy indicates that the proposed method applies to the zone between the Arctic Circle ($+66.3^\circ$ latitude) and the Antarctic Circle (-66.3° latitude). Given that most of the world's population/industrial activity is concentrated in this region, the method was considered to be satisfactory.

Furthermore, it is emphasised that some other important considerations were made in the course of this work. For instance, the possible mechanical

limitations of the inclination that radiation-tracking structures could assume for two axes were not considered. The fixed surfaces were considered to have an identical inclination compared to the local latitude.

In summary, the aim of this section is to develop a proposed process of determining the solar energy incident on a capturing surface for a specific location, date, and time in temperate and intertropical latitudes. A comparison of the results obtained with real data recorded in databases that are available for performance authentication, as well as the estimation of the energy gain between the types of incidence surfaces is performed.

3.2 CALCULATION METHOD

The proposed method for estimating the solar energy incident on a capturing surface is summarised in Table 1. In the presented step-by-step process, the equation for the calculation of the incident energy is displayed for an interval of 1 h. The process must be interactive to calculate the accumulated daily and annual energy, based on Eq. 14. As an illustration, the estimated values for the city of Vitória, ES, Brazil, are presented for the period between 11:00 and 12:00 on the first day of the calendar year (January 1st).

The independent variables of the system are the latitude, longitude, and altitude of the location under analysis. At each interaction, the value of the energy incident at that instant, day, and time, for each of the three types of receiving surface of interest is obtained. Processing is performed with a one-hour step, covering 365 days of the year.

Table 1: Descriptive itinerary of the proposed method for calculating solar energy incident on fixed flat surfaces, uniaxial solar trackers, and biaxial solar trackers

Step	Parameter	Determination Method	Typical Result
1	Location	Arbitrary	Vitoria, Brazil
	Latitude		-20.3222°
	Longitude		-40.3381°
	Altitude		4 m
	Reference meridian		Depending on the hemisphere location
2	Solar Constant	(GUEYMARD, 2018)	1,361.1 W/m ²
	Day of the year		Jan. / 1 st
3	Start Hour	Arbitrary	Sunrise – 5:00
	Final Hour		Sunset – 18:00
4	Daily angle of interaction between the Sun and the Earth - Γ	Equation 2	0 rad
5	Declination of the terrestrial axis - δ	Equation 3	-0.402449 rad
6	Earth orbit eccentricity correction factor - E_0	Equation 1	1.03505 rad
7	Time Correction - E_t	Equation 5	-0.0127395
8	Solar Time	Equation 4	11.45 h
9	Time Angle - ω	Equation 6	-0.14390 rad
10	Zenith Angle - θ_z	Equation 7	0.14190 rad
11	Azimuth Solar Angle - γ_s	Equation 8	-1.2015 rad
12	Angle of incidence on a fixed surface - θ_{fixed}	Equation 9	0.91055 rad
13	Angle of incidence on a uniaxial tracking surface - θ'	Equation 10	0.91055 rad
14	Azimuth angle of the uniaxial surface - γ	Equation 10	0.39512 rad
15	Inclination angle of uniaxial surface - β	Equation 11	-0.38161 rad
16	Inclination angle of uniaxial surface - θ_{1Ex}	Equation 11	0.92005 rad
17	Azimuth angle of the uniaxial surface - γ	$\gamma = \gamma_s$	-1.2015 rad
18	Inclination angle of biaxial surface - β	$\beta = \theta_z$	0.14190 rad
19	Angle of incidence on a biaxial tracking surface - θ''	Equation 17	1.0000 rad
20	Irradiance on a fixed surface - I_{fixed}	$I_{fixed} = I_{cs} E_0 \cos(\theta_{fixed})$	1,282.79 Wh/m ²
21	Irradiance on a uniaxial surface - I_{1Axis}	$I_{1Axis} = I_{cs} E_0 \cos(\theta')$	1,296.17 Wh/m ²
22	Irradiance on a biaxial surface - I_{2Axes}	$I_{2Axes} = I_{cs} E_0 \cos(\theta'')$	1,408.81 Wh/m ²
23	Air Mass Factor - $AM(\theta_z)$	Equation 13	1.0053
24	Energy Incident on the fixed surface due to Air Mass - B	Equation 14	901.56 Wh/m ²
25	Energy Incident on the uniaxial surface due to Air Mass - B	Equation 14	910.96 Wh/m ²
26	Energy Incident on the biaxial surface due to Air Mass - B	Equation 14	990.12 Wh/m ²

4 RESULTS AND DISCUSSION

4.1 COMPARISON OF THE RESULTS FOR THE ESTIMATION OF THE INCIDENT SOLAR ENERGY WITH EXISTING DATABASES

The method proposed in Section 3.2 can be used in a multitude of geographical coordinates. In order to analyse the results obtained, the National Solar Radiation Database (NREL) (NATIONAL RENEWABLE ENERGY LABORATORY (NREL), [s.d.]) was used for comparison with the values estimated in this study research.

The NREL contains meteorological data collected from different regions and at different periods, and its information set covers almost the entire American continent (Arctic Circle to the Tropic of Capricorn).

As a means of comparison, a city located within the Intertropical Zone (Vitoria, Brazil), a city located close to the equator region (Quito, Equator), and a city positioned within the Temperate Zone (Vancouver, Canada) were chosen. Table 2 presents the relevant geographical particularities of each of these cities.

Table 2: Target cities and their geographical particularities

City	Latitude	Longitude	Altitude
Vitoria	-20.3222°	-40.3381°	4 m
Quito	-0.2252°	-78.5248°	2,908 m
Vancouver	49.3023°	-123.1070°	105 m

The data set extracted from the NREL was the direct normal irradiance towards a “clear sky” and as such, the data were compared to the estimated irradiance for a two-axis tracking surface because the objective is to describe the same phenomenon: a surface with normal incident solar radiation throughout the day.

The metric used for performance analysis of the proposed method was its mean error with regard to the data in the NREL database.

The results of the calculated errors are shown in Table 3. It appears that the proposed model results in an average error for monthly annual forecasts of solar energy incidence of approximately 4% for cities with different latitudes. This is considered to be a low prevision error with low bias. Moreover, given the final goal of achieving a comparative value of incident solar energy for different surfaces submitted to the same conditions, such errors are minimised via this process of evaluation (mathematical division). Thus, it is understood that the proposed model is suitable for the intended purposes.

Table 3: Estimation errors for the proposed model with respect to the reference database

City	Month Mean Error	Annual Mean Error
Vitoria	+4.3%	+4.3%
Quito	+4.9%	+4.8%
Vancouver	-4.4%	-2.6%

4.2 ENERGY ANALYSIS OF TRACKING SURFACES

Analogous to the previous sections, the cities of Vitoria, Quito, and Vancouver will be analysed in terms of the energy gain of the tracking surfaces compared to a conventional fixed surface and the comparative gain between them.

4.2.1 Energy analysis of Vitoria, Brazil

The results for the city of Vitoria can be interpreted based on Figure 2. This graph shows the energy capture gains for uni- and biaxial solar trackers compared to the fixed surface, with daily resolution, that is, the points that make up the graph represent the accumulated gain day by day of the year. Below, monthly gains are analysed, that is, the accumulated gain month by month throughout the year.

It is seen that the tracking surfaces for one axis have an advantage of approximately 45% in the summer months (December to March) and 28% in the

winter months (June to September), related to fixed surface. However, the surfaces with biaxial movements in these even months show gains close to 55% and 40%, respectively, in regard to the fixed surfaces.

Results from simulation show that fixed surfaces contribute approximately 2.2 MWh/m² per year, whereas surfaces with tracking structures with one axis and surfaces with two-axis tracking contribute 3.0 MWh/m² and 3.1 MWh/m², respectively. Therefore, the annual gain of the tracking surfaces compared to a surface supported on a fixed structure for tracking using one axis, 36.4%, and for tracking using two axes, 42.4%. Moreover, the two axes tracking surfaces exhibit a gain of 4.4% compared to those with only one axis.

By analysing the results for the surfaces with biaxial movements relative to those with only one degree of freedom as shown in Figure 2, it is noted that the greatest increase in the irradiance occurs close to the period of summer and winter solstices, reaching a maximum value of 9%. It is also noticed that there are no significant gains for the biaxial surfaces during the periods close to the equinoxes.

4.2.2 Energy analysis of Quito, Equator

For the city of Quito, the uniaxial surface has an annual gain of 37.9% relative to the fixed surfaces. The biaxial surface has a gain of 43.8% relative to fixed surfaces and 4.3% with respect to single-axis trackers.

When analysing the gain of tracking surfaces with two axes compared to trackers with one axis, a behaviour similar to that of the city of Vitoria is observed both in terms of the maximum and minimum gains, and during the period for which they occur: approximately 9% for the period of the solstice and a minimum of 0% during the period of the equinox.

4.2.3 Energy analysis of Vancouver, Canada

In conclusion, the irradiance associated with the city of Vancouver was analysed, which revealed that this case was substantially different from the others, depicting impressive gains of approximately 62% for uniaxial tracking surfaces and a large increase of 77% for biaxial surfaces compared to fixed surfaces. Reasonable gains of approximately 18% for uniaxial surfaces and 28% for biaxial surfaces can also be realized during the winter period.

The peculiarities of irradiance over a city located in a temperate zone expire when the percentage addition of irradiance from a biaxial plane is investigated in comparison to a uniaxial plane.

In comparison, the structure with one axis has an annual gain of approximately 42.1% whereas that with two axes has a gain of 47.4%, relative to a fixed structure. With regard to the tracking surfaces, the two axes surfaces have a 3.7% gain relative to the surface with only one axis.

Table 4 summarises the previously presented results for the energy gain in the three investigated cities.

5 CONCLUSIONS

The method proposed in this work facilitates the estimation of energy gain during the capture of solar energy by uni- and biaxial solar tracking surfaces with regard to fixed surfaces, depending on the location of interest and the day of the year. This tool can be used for technical-economic feasibility analysis of the type of surface required for solar energy projects, and the analysis of the performance of these systems in operation. In addition, it is useful for a range of applications including the planning of maintenance interventions and the shutdown of tracking systems during periods of low energy gain.

Unlike empirical or typical approaches, the recommended method can

be used in any location of interest to obtain specific estimates for that region according to the altitude and specific geographic coordinates.

Regarding the gains in solar energy capture as a function of latitude, it is noted that the greater the latitude, the further the location is away from the equator, the greater the annual gain by increasing the fixed surface for uni- or biaxial solar trackers. The greater the latitude, the

greater the variation in the incidence angle of solar radiation on the energy capture surface, which reduces solar energy capture. By using solar trackers, this variation is minimized.

The presented approach can be easily implemented using computational iterative algorithms, which will encourage widespread use. In this study, Python was used as the programming language, which requires low computational effort.

Figure 2: Daily energy gain of biaxial tracking surfaces in relation to uniaxial surfaces for Vitoria

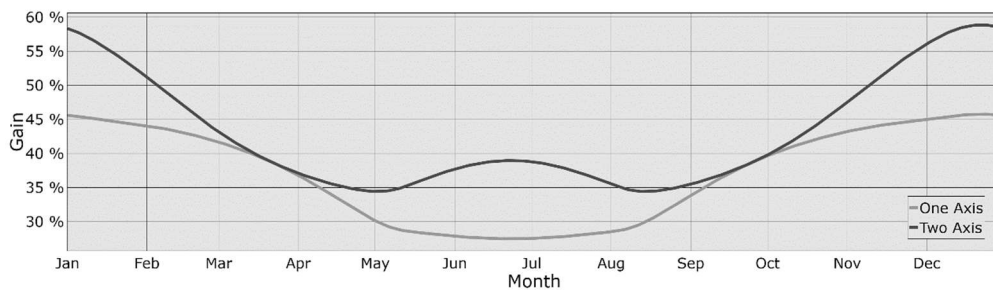


Table 4: Monthly and annual relative energy gain depending on the incidence surface in addition to fixed and uniaxial surfaces

Reference Surface	Tracking	Gain Type	Cities		
			Vitoria	Quito	Vancouver
Fixed	Uniaxial	Maximum monthly	45.0%	38.0%	62.0%
		Minimum monthly	28.0%	37.0%	18.0%
		Annual	36.4%	37.9%	42.1%
	Biaxial	Maximum monthly	55.0%	38.0%	77.0%
		Minimum monthly	40.0%	49.0%	28.0%
		Annual	42.4%	43.8%	47.4%
Uniaxial	Biaxial	Maximum monthly	9.0%	9.0%	9.0%
		Minimum monthly	0.0%	0.0%	0.0%
		Annual	4.4%	4.3%	3.7%

ACKNOWLEDGEMENTS

Funding: This work was partially supported by the Instituto Federal do Espírito Santo, Brazil [Notice Ifes PRPPG 07/2020].

NOTATION

The following symbols are used in this paper:

d_n an arbitrary day of the year, [-]

E_0	correction factor for solar constant, [rad]
E_t	correction of the duration of a day, [rad]
I	irradiance at the top of the Earth's atmosphere, [Wh/m ²]
I_{cs}	incident solar radiation in to a plane, [Wh/m ²]
L_{local}	local latitude, [rad]
L_{ref}	reference latitude, [rad]
SC	solar constant, [W/m ²]
ST	solar time, [min]
TSI	total solar irradiance, [W/m ²]
α_s	solar altitude angle, [rad]
β	slope angle, [rad]
γ	azimuth angle, [rad]
γ_s	solar azimuth angle, [rad]
Γ	day angle, [rad]
δ	solar declination angle, [rad]
θ	incidence angle, [rad]
θ_z	zenith angle, [rad]
φ	latitude angle, [rad]
ω	time angle, [rad]

REFERENCES

- ABDELGHANI-IDRISSI, M. A. et al. Solar tracker for enhancement of the thermal efficiency of solar water heating system. **Renewable Energy**, v. 119, p. 79–94, 2018.
- AL-RAWAHI, N. Z.; AL-AZRI, N. Z. Effect of latitude and sky clearance factor on the effectiveness of solar tracking strategies. **Cogent Engineering**, v. 6, n. 1, 2019.
- ALLAM, E. **7 Most Popular Solar PV Design and Simulation Software**. Disponível em: <<https://www.linkedin.com/pulse/7-most-popular-solar-pv-design-simulation-software-eslam-allam>>. Acesso em: 20 jul. 2020.
- ANTONANZAS-TORRES, F. et al. Clear sky solar irradiance models: A review of seventy models. **Renewable and Sustainable Energy Reviews**, v. 107, n. March 2018, p. 374–387, 2019.
- AWASTHI, A. et al. Review on sun tracking technology in solar PV system. **Energy Reports**, v. 6, p. 392–405, 2020.
- BAGGIO, F. A. V. **Economic Analysis of Micro And Mini Distributed Geration Using Photovoltaic Panels (In Portuguese)**. VI Congresso Brasileiro de Energia Solar. **Anais...**Belo Horizonte: 2016Disponível em: <Associação Brasileira de Energia Solar>
- BAHRAMI, A.; OKOYE, C. O.; ATIKOL, U. The effect of latitude on the performance of different solar trackers in Europe and Africa. **Applied Energy**, v. 177, p. 896–906, 2016.
- BATAYNEH, W. et al. Investigation of a single-axis discrete solar tracking system for reduced actuations and maximum energy collection. **Automation in Construction**, v. 98, n. November 2018, p. 102–109, 2019.
- BEHAR, O. et al. Critical analysis and performance comparison of thirty-eight (38) clear-sky direct irradiance models under the climate of Chilean Atacama Desert. **Renewable Energy**, v. 153, p. 49–60, 2019.
- BRAUN, J. E.; MITCHELL, J. C. Solar geometry for fixed and tracking surfaces. **Solar Energy**, v. 31, n. 5, p. 439–444, 1983.
- BROWNSON, J. R. S. **Solar Energy Conversion Systems**. 1. ed. Boston: Academic Press, 2014.
- CLIFFORD, M. J.; EASTWOOD, D. Design of a novel passive solar tracker. **Solar Energy**, v. 77, n. 3, p. 269–280, 2004.
- COFFARI, E. The Sun and the Celestial Vault. In: SAYIGH, A. A. M. B. T.-S. E. E. (Ed.). **Solar Energy Engineering**. [s.l.] Elsevier, 1977. p. 5–36.
- DE MACEDO, M. M.; SALDIAS, C. E. P.; ANDO JUNIOR, O. H. Mathematical Modeling of a Solar Tracker System Two Axes for Generation Photovoltaics. **IEEE**

- Latin America Transactions**, v. 14, n. 9, p. 4054–4062, set. 2016.
- DUFFIE, J. A.; BECKMAN, W. A. **Solar Engineering of Thermal Processes**. 4. ed. New Jersey: John Wiley & Sons, Inc., 1985. v. 53
- FATHABADI, H. Comparative study between two novel sensorless and sensor based dual-axis solar trackers. **Solar Energy**, v. 138, p. 67–76, 2016.
- FRÖHLICH, C.; LEAN, J. Solar radiative output and its variability : evidence and mechanisms. **The Astronomy and Astrophysics Review**, v. 12, n. 4, p. 273–320, 2004.
- GUEYMARD, C. A. A reevaluation of the solar constant based on a 42-year total solar irradiance time series and a reconciliation of spaceborne observations. **Solar Energy**, v. 168, n. March, p. 2–9, 2018.
- HAFEZ, A. Z.; YOUSEF, A. M.; HARAG, N. M. Solar tracking systems: Technologies and trackers drive types – A review. **Renewable and Sustainable Energy Reviews**, v. 91, n. June 2017, p. 754–782, 2018.
- IQBAL, M. **An Introduction To Solar Radiation**. 1. ed. Vancouver, British Columbia, Canada: Academic Press, 1983.
- KASBURG, C.; FRIZZO STEFENON, S. Deep Learning for Photovoltaic Generation Forecast in Active Solar Trackers. **IEEE Latin America Transactions**, v. 17, n. 12, p. 2013–2019, 2019.
- KASTEN, F.; YOUNG, A. T. Revised optical air mass tables and approximation formula. **Applied Optics**, v. 28, 1989.
- KUHN, J. R.; ARMSTRONG, J. D. Mechanisms of solar irradiance variations. In: [s.l: s.n.]. p. 87–96.
- MEINEL, A. B.; MEINEL, M. P. Applied solar energy: An introduction. **NASA STI/Recon Technical Report A**, v. 77, p. 33445, jan. 1977.
- NATIONAL RENEWABLE ENERGY LABORATORY (NREL). **NSRDB Data Viewer**. Disponível em: <<https://maps.nrel.gov/nsrdb-viewer>>. Acesso em: 17 maio. 2020.
- PAP, J. Variation of the Solar Constant During the Solar Cycle. **Astrophysics and Space Science**, v. 127, n. 1, p. 55–71, 1986.
- PINHO, J. T.; GALDINO, M. A. **Manual de Engenharia Para Sistemas Fotovoltaicos**. Rio de Janeiro, Brasil: [s.n.].
- RECA-CARDEÑA, J.; LÓPEZ-LUQUE, R. Chapter 9 - Design Principles of Photovoltaic Irrigation Systems. In: YAHYAOU, I. B. T.-A. IN R. E. AND P. T. (Ed.). . **Advances in Renewable Energies and Power Technologies**. [s.l.] Elsevier, 2018. p. 295–333.
- RIGOLLIER, C.; BAUER, O.; WALD, L. On the clear sky model of the ESRA — European Solar Radiation Atlas — with respect to the heliosat method. **Solar Energy**, v. 68, n. 1, p. 33–48, jan. 2000.
- SIDEK, M. H. M. et al. Automated positioning dual-axis solar tracking system with precision elevation and azimuth angle control. **Energy**, v. 124, p. 160–170, 2017.
- SPENCER, J. W. Fourier series representation of the position of the sun. **Search**, v. 2, n. 5, p. 172+, 1971.
- SPROUL, A. B. Derivation of the solar geometric relationships using vector analysis. **Renewable Energy**, v. 32, n. 7, p. 1187–1205, 2007.
- UNGURESAN, P. V. et al. Orientation of Facades for Active Solar Energy Applications in Different Climatic Conditions. **Journal of Energy Engineering**, v. 143, n. 6, p. 1–11, 2017.
- USOSKIN, I. G. A history of solar activity over millennia. **Living Reviews in Solar Physics**, v. 14, n. 1, p. 3, 2017.
- XU, H. et al. Experimental Investigation on a Photovoltaic Thermal Solar System

with a Linear Fresnel Lens. **Journal of Energy Engineering**, v. 144, n. 3, p. 1–10, 2018.

ZHU, Y.; LIU, J.; YANG, X. Design and performance analysis of a solar tracking system with a novel single-axis tracking structure to maximize energy collection. **Applied Energy**, v. 264, n. February, p. 114647, abr. 2020.